Power Optimal Control Allocation for Distributed Electric Propulsion in a Series/Parallel Hybrid Powertrain

Jonathan S. Litt[1]
NASA Glenn Research Center, Cleveland, OH, 44135, USA

This paper describes a thrust allocation scheme that minimizes power consumption in an electrified powertrain with Distributed Electric Propulsion. It takes advantage of an observation about component efficiency maps, that efficiency is often highest at high torque/high speed conditions. This optimal approach is demonstrated to satisfy total thrust and net yaw axis torque requirements, making it suitable for utilizing differential thrust for maneuvering.

I. Introduction

Electrification of aircraft powertrains is being investigated as a way to make air travel more efficient. Electrification provides multiple aerodynamic benefits depending upon the architecture and configuration [1]. For instance, an electrified aircraft powertrain with Distributed Electric Propulsion (DEP), i.e., a powertrain with at least one power source and electric fans that produce thrust, provides an increased effective bypass ratio of the whole propulsion system compared to conventional propulsion systems, enabling higher propulsive efficiency [2]. The NASA concept SUbsonic Single Aft eNgine (SUSAN) Electrofan aircraft [3] has a series/parallel partial hybrid architecture (Figure 1). This means that the engine from which power is extracted to drive the fans also produces thrust. The powertrain should be designed to be most efficient at the operating point at which it spends the most time, e.g., cruise. That being said, there are potentially additional optimizations to be made regarding how the system is used that improve efficiency further. In Ref. [4], a power savings was demonstrated compared to the baseline control by assuming that the efficiency of each electrical string (the power flow path consisting of the components from the generator to the fan motor) was known, then allocating thrust commands according to an optimal control solution. This approach assumed that the string efficiencies were fixed but randomly distributed between 90% and 99% due to manufacturing variations. A more realistic representation is that the efficiency variation depends on operating condition, i.e., speed and torque. A notional motor efficiency map is shown in Figure 2. Here efficiency increases as the motor goes to higher speeds and higher torques.

Figure 3 [4] demonstrates the relationships between variables related to the thrust producing fans distributed along the wings in the SUSAN aircraft. It can be seen that at a given operating point, there is a linear relationship between thrust and power. It is also clear that for any value of thrust, for instance, there is a corresponding value for

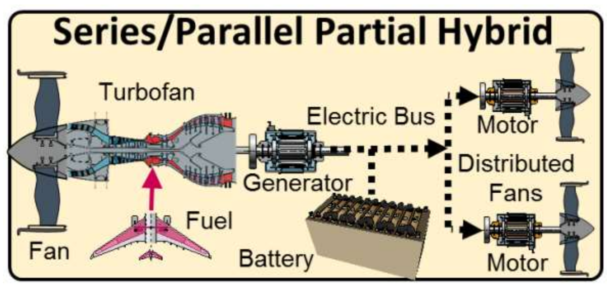

Figure 1. Series/parallel partial hybrid powertrain architecture.

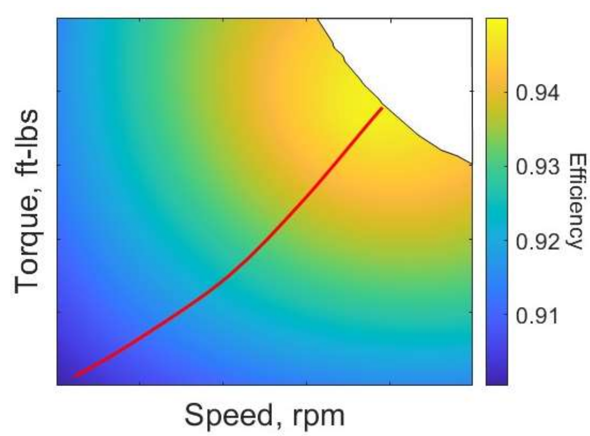

Figure 2. Notional motor efficiency map showing fan cruise operating line.

[1]Aerospace Engineer, Intelligent Control and Autonomy Branch, AIAA Associate Fellow

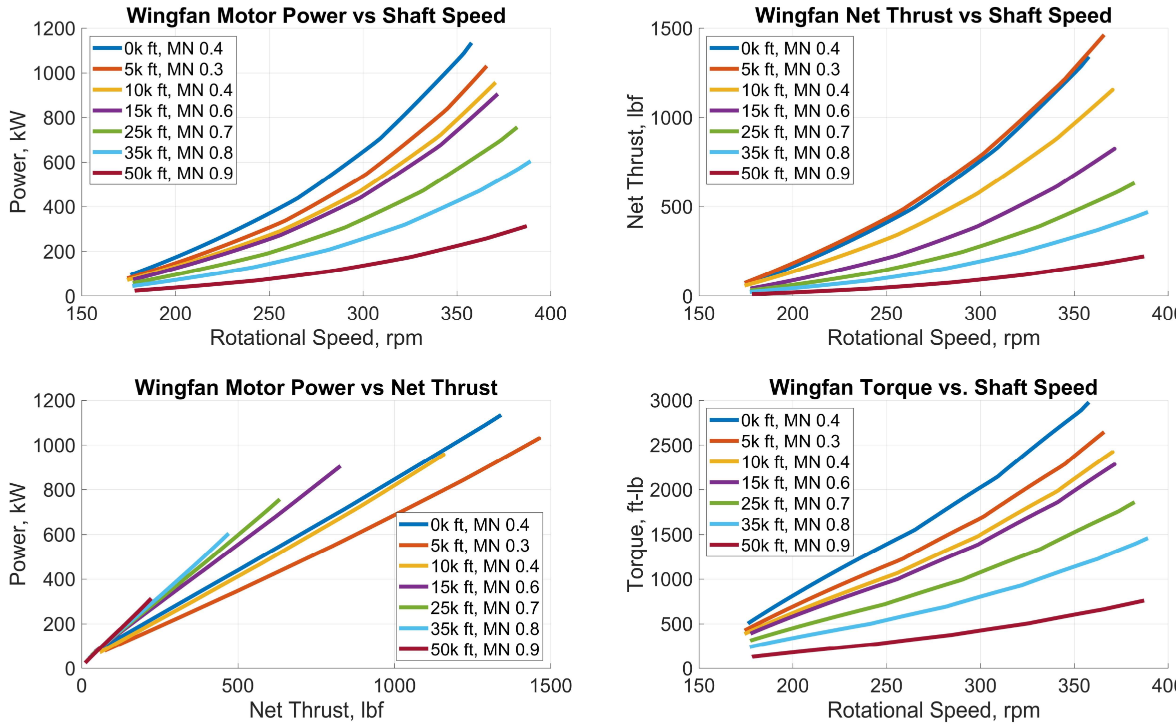

Figure 3. Motor power, net thrust, and motor torque vs fan rotational speed, and motor power vs net thrust at various flight conditions for a SUSAN wingfan.

each of the other variables. If one were to overlay the torque vs. rotational speed plot (lower right plot in Figure 3) on a motor efficiency map (Figure 2), it is reasonable to expect that the cruise curve (35,000 ft, Mach 0.8) would pass from the lower efficiency region through the area of highest efficiency at the upper end of the speed range.

The rest of this paper is as follows: The next section describes the development of the concept behind the optimal control approach. After that, the optimal control problem statement is presented, followed by several illustrative examples. Subsequent sections include a Discussion and Conclusions.

II. Concept

Electrical components for electrified aircraft powertrains should be optimized for overall system-level benefits, so it is not unreasonable to assume that a map similar to that in Figure 2 could be generated for a complete electrical string. In other words, the most efficient operating points of all components in the string will approximately coincide by design, resulting in the region of highest efficiency being situated at the upper right of the operating range. Given this assumption, an efficiency curve such as that in Figure 4 can be developed by plotting the torque vs. speed points (from the lower right plot in Figure 3) on the efficiency map of the complete electrical string (similar to the red curve in Figure 2) against the corresponding thrust values at the cruise operating point. This produces a plot of efficiency over the range of cruise thrust values. Looking at the power vs. thrust plot (lower left) in Figure 3, an output power is determined for every thrust value. This output power divided by the string efficiency at that thrust value (Figure 4) gives the input power required, and the difference is the power loss (Figure 5). Because the power consumed at low thrust is low, even though the efficiency is lower than at higher thrust, the power lost is less than at higher power. In Figure 4, the efficiency approaches 95% asymptotically, thus the power loss increases almost linearly as thrust increases at the high end but drops off rapidly as thrust decreases at the lower end (Figure 5). Now, the objective is to determine the control approach that minimizes power consumption.

III. Problem Statement

Based on the curve in Figure 5, a fan that produces the minimum thrust will be penalized proportionally less in terms of absolute power consumption than one that produces more thrust. This leads to the conclusion that having as many fans as possible at the minimum thrust level while still allowing the overall thrust demand to be met will save

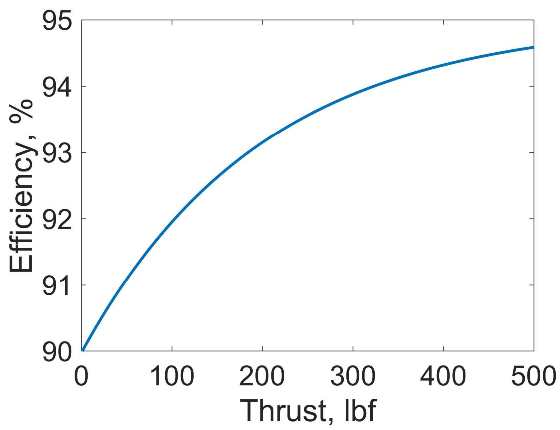

Figure 4. Notional efficiency plot corresponding to the map in Figure 2 for a cruise condition.

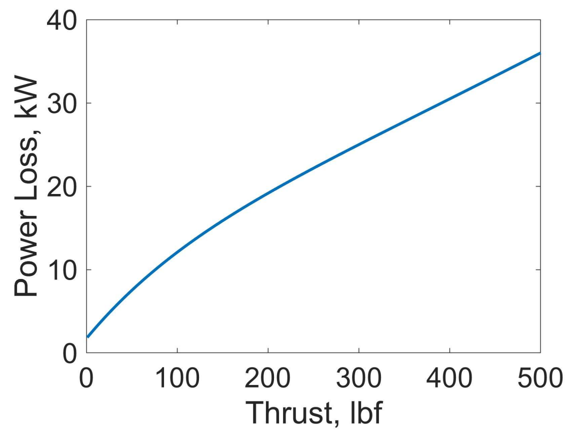

Figure 5. Power Loss vs. Thrust curve for a single wingfan.

the most power. The implication of this, using constrained linear programming, is that as many of the remaining fans as possible must be at maximum power while still achieving the demanded total net thrust and net torque about the vehicle yaw axis, which must be zero unless differential thrust is required for turning [4].

IV. Examples

The examples use cruise data (35k ft, MN 0.8) from the SUSAN wingfan (Figure 3) and the efficiency curve from Figure 4. The assumption is that the efficiency increases monotonically, and its slope decreases with increased thrust.

$$efficiency = 0.95\, e^{-thru \quad /200}$$

The DEP system has 16 wing-mounted fans (wingfans), eight under each wing, in a mail slot configuration (Figure 6). The wingfans are evenly positioned at a distance from the aircraft's longitudinal axis (Figure 7). When the wingfans are used differentially, the resulting thrust asymmetry creates a yaw moment on the aircraft similar to the function of the rudder. Each wingfan has a thrust range from 26 lbf (idle) to 500 lbf (maximum power). Wingfan mechanical power is the product of the motor shaft's speed and delivered torque. This power divided by the electrical string efficiency gives the input power required. The difference between input electrical power and output shaft power is the power loss. In the following examples, wingfan thrust setpoints are determined such that both the total thrust and net torque demands on the aircraft are met.

Figure 6. SUSAN showing the 16 wingfans in a mail slot configuration under the wings.

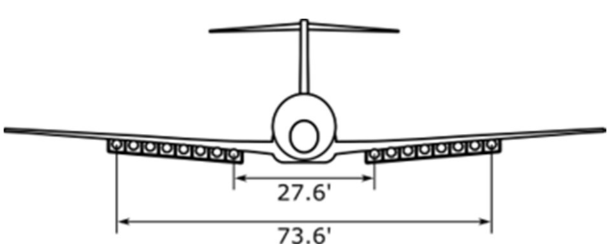

Figure 7. SUSAN front view showing wingfan locations. The measurements indicate that the wingfans are spaced about 3.3 ft on center.

A. Example 1: Single Cruise Point

For the first example, a total thrust of 5156 lbf was demanded with zero net torque about the yaw axis. 10,000 cases were simulated. For each trial, thrust values within the allowable range (26-500 lbf) were assigned randomly with a uniform distribution to 14 of the 16 wingfans, selected at random. The thrust setpoints of the remaining two were set to meet the total thrust and net yaw axis torque requirements, if possible, otherwise a new set of thrusts was assigned until a feasible set was achieved. Based on the thrust values, a total power loss was computed (Figure 8). Also shown in Figure 8 is the 10,001st case, in which all wingfans produced the same

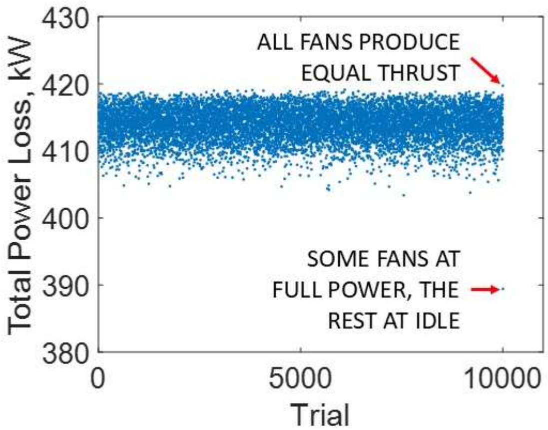

Figure 8. Example 1: Total power lost in 10,000 random scenarios, plus one case with all fans equal, and one case with some at full power and the rest at idle.

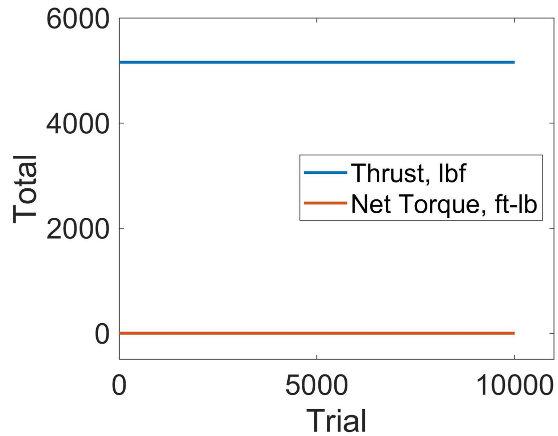

Figure 9. Example 1: Same cases shown in Figure 8 demonstrating that they all produce the same total thrust and net yaw axis torque.

thrust (5156/16 lbf), and the 10,002nd case in which 10 wingfans were at full power and six were at idle. The case in which all wingfans produced the same thrust consumed the most power by a small amount. The hypothesized optimal solution consumed significantly less power than any other case. Finally, as a check, Figure 9 shows that both the total thrust and net torque about the yaw axis meet the requirements for all cases.

Two more examples (Examples 2 and 3) are now presented using the coordinated turn data from Ref. [4], also at the cruise condition. Example 2 maintains only the total net thrust requirement, assuming no differential thrust. This symmetry about the yaw-axis makes clear how this control, which is essentially bang-bang, works. Example 3 maintains the requirements on both the total net thrust and net torque about the yaw axis, which performs a coordinated turn using the electric propulsors to provide a yaw moment to the vehicle.

B. Example 2: Cruise Thrust Level Change

In this example, dynamic total net thrust data across a range of power levels from Ref. [4] is used. Here, the optimal approach is compared to the case in which all wingfans produce the same thrust, i.e., one-sixteenth of the total (Figure 10). For the optimal case, it is instructive to look at Figure 11, which shows the total thrust over time superimposed on a plot of the maximum number of wingfans that can be at full power. Because the thrust on the two wings balances, there is no torque about the yaw axis and no tendency to turn. To maintain this balance, the corresponding wingfans

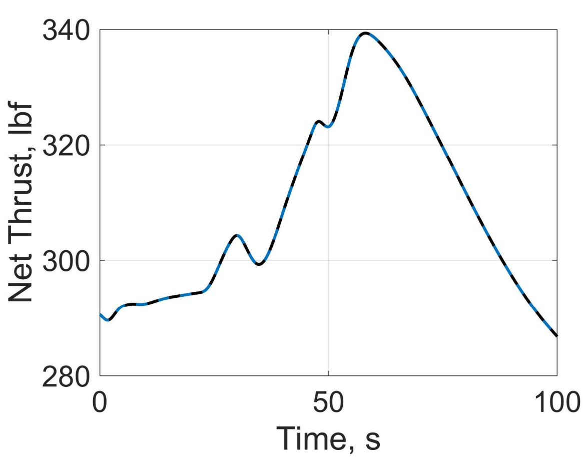

Figure 10. Example 2: Individual baseline identical wingfan thrusts. All 16 thrust plots exactly coincide.

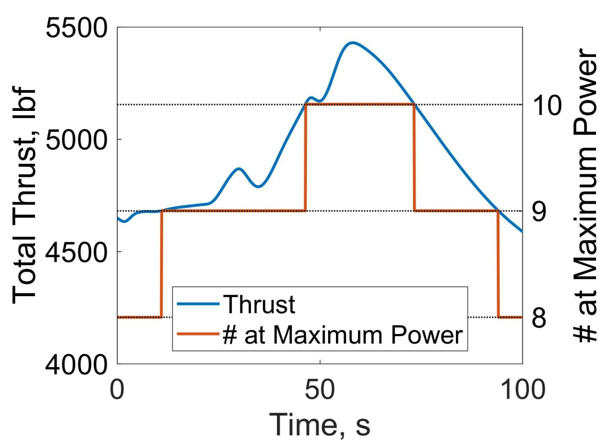

Figure 11. Example 2: Thrust and number of wingfans that can be at full power.

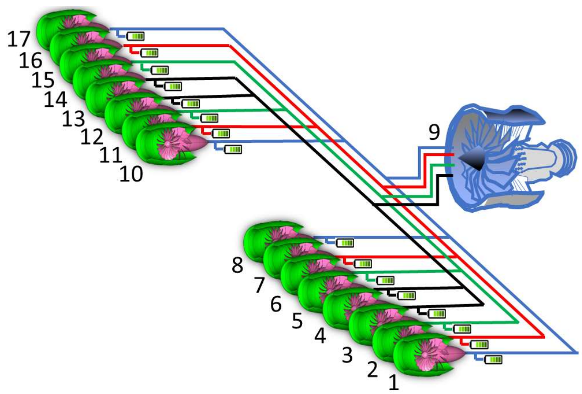

Figure 12. SUSAN powertrain showing engine numbering. Port side wingfans are numbered 1-8 left to right, the turbofan engine is #9, and the starboard side wingfans are 10-17 left to right from the pilot's point of view.

on opposite sides operate in synchronized fashion. The wingfan numbering is shown in Figure 12. Figure 13 shows the wingfan commands over time. It is clear that when, based on the thrust level, the maximum number that can be at full power (refer to Figure 11) is eight, the eight center fans (four on each side) are at full power, the six (three on each side) further out are at idle, and the two outermost move in unison to achieve the total thrust. Once the maximum number that can be at full power increases to nine, the last two wingfans account for that between them, as well as the remaining thrust demand. When the maximum number that can be at full power increases to 10, wingfans 4 and 14 immediately increase to full power while wingfans 1 and 17 immediately decrease but then continue to track the remaining thrust demand. As the thrust demand decreases, the commands to wingfans 4 and 14 drop to the lower limit while those to wingfans 1 and 17 jump up, maintaining a continuous

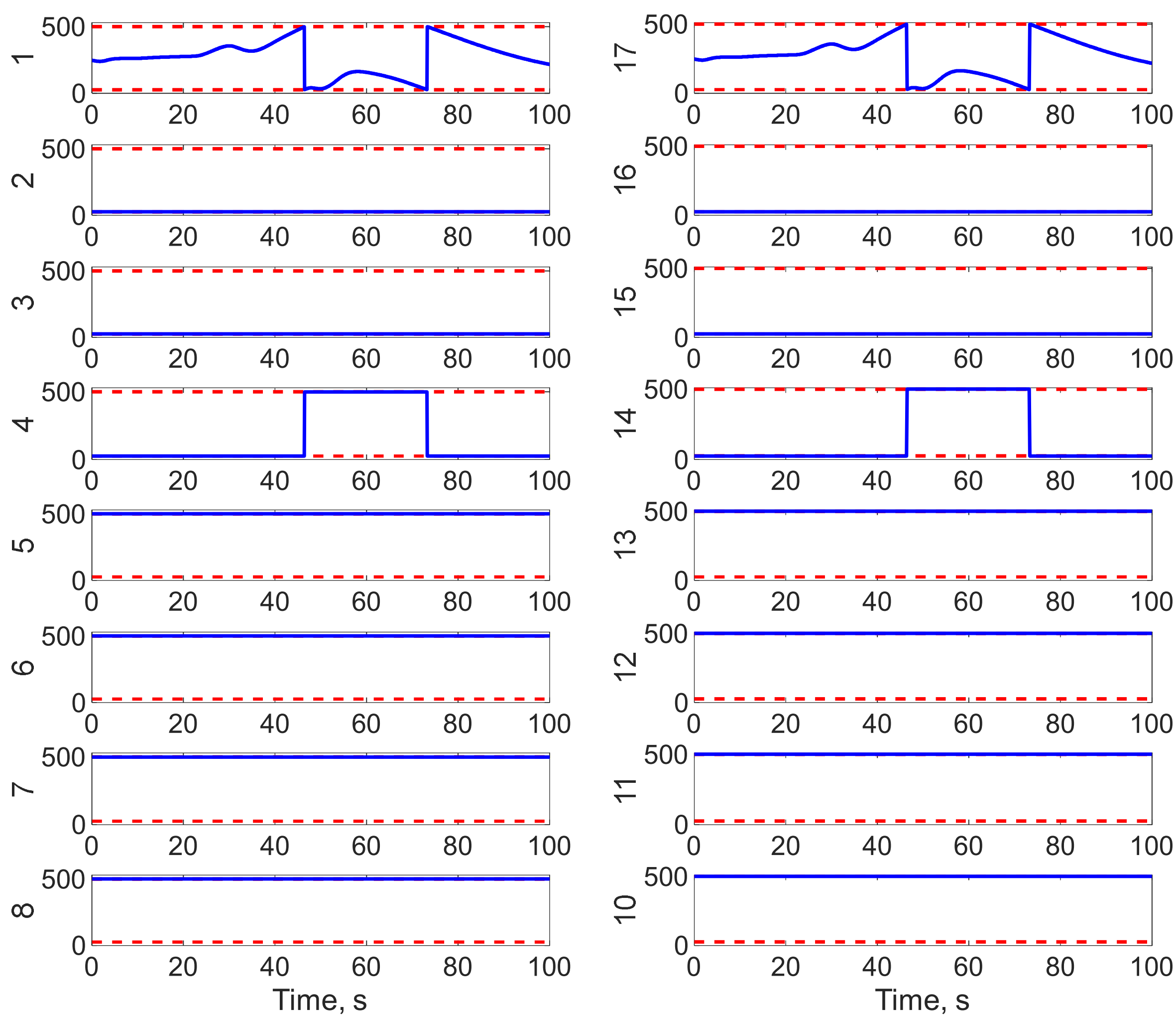

Figure 13. Example 2: Thrust commands for case with zero net torque about the yaw axis. Numbered plots correspond to outermost to innermost wingfans top to bottom (refer to Figure 12). Dashed lines indicate upper (500 lbf) and lower (26 lbf) limits.

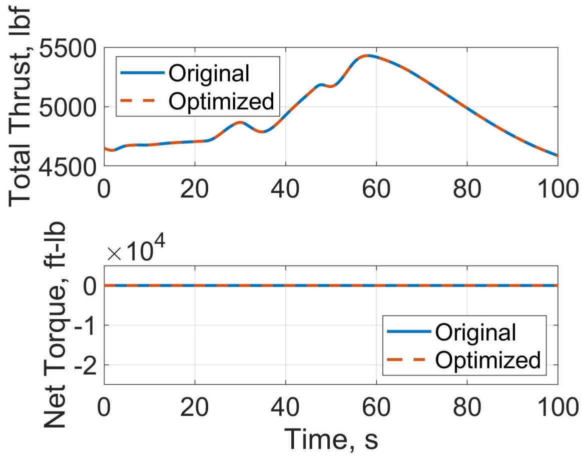

Figure 14. Example 2: Total thrust and net yaw axis torque due to original and optimized commands.

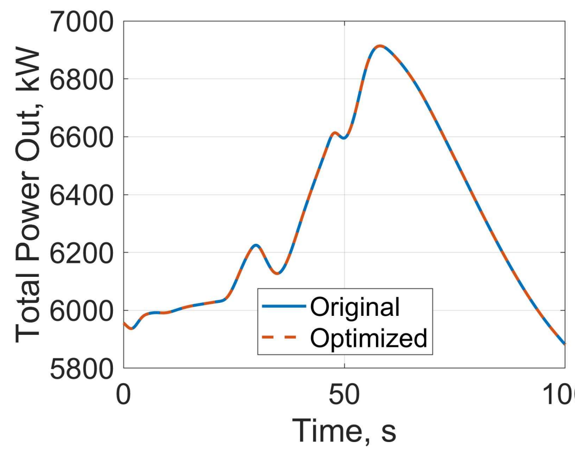

Figure 15. Example 2: Total output power for example with no differential thrust.

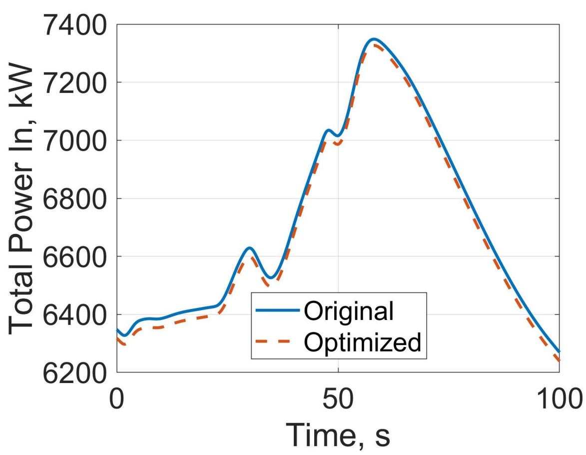

Figure 16. Example 2: Total input power for example with no differential thrust.

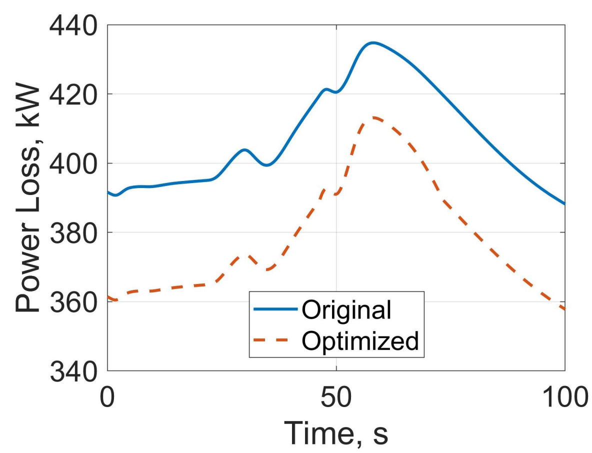

Figure 17. Example 2: Power loss for example with no differential thrust.

overall thrust demand, then decrease together slowly. Clearly, because symmetry is being maintained, there are always an even number of wingfans at full power, with the two sides mirror images of each other. The outermost wingfans working together deliver the thrust that a single fan is capable of when operating in the lower half of their range, and that of between one and two at full power when operating in the upper half of their range. Figure 14 shows how the optimized commands result in matching the thrust and net yaw axis torque of the original. The output power for both cases is shown in Figure 15; they match because the total thrust matches and there is a linear relationship between thrust and power (the power of the total thrust equals the sum of the powers of the individual thrusts). However, because the optimized case is more efficient, the power extracted from the turbofan to achieve the required thrust is less (Figure 16). The power loss over time for both cases is shown in Figure 17. The power savings represents about 0.3-0.4% of the total with a slightly smaller reduction at higher power.

C. Example 3: Coordinated Turn Using Differential Thrust to Replace the Rudder Function

In this example, the coordinated turn using DEP from Ref. [4] is replicated. The individual thrust commands from the flight control [5] are shown in Figure 18. Note that the total thrust (the sum of the individual thrust demands) is the same as in the previous example. The optimal commands that produce the same total thrust and net torque about the yaw axis are shown in Figure 19. The commands start out the same as in the previous example but deviate once the net torque about the yaw axis becomes nonzero at about 20 seconds (Figure 20). The asymmetry in the commands results from the requirement to match the nonzero torque demand about the yaw axis for the turn. Figure 20 shows

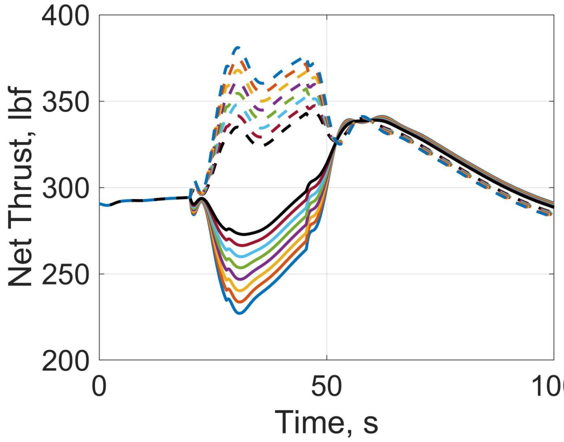

Figure 18. Example 3: Differential thrusts for a coordinated turn.

that the wingfan commands are able to match the result of the original commands (Figure 18) but requiring less power (Figure 21). Again, the mechanical power is the same (Figure 22), but the optimal commands result in less power loss (Figure 23). While the pattern of thrust commands is more complicated here than in the previous example, the total is the same at every point in time, only the yawing moment due to the thrust asymmetry varies, which is how the turn is accomplished.

V. Discussion

There are several observations to be made about the examples. In general, the wingfan commands to achieve the desired thrust and net yaw axis torque are not unique. For instance, in the second example the center (innermost) wingfans were used to provide most

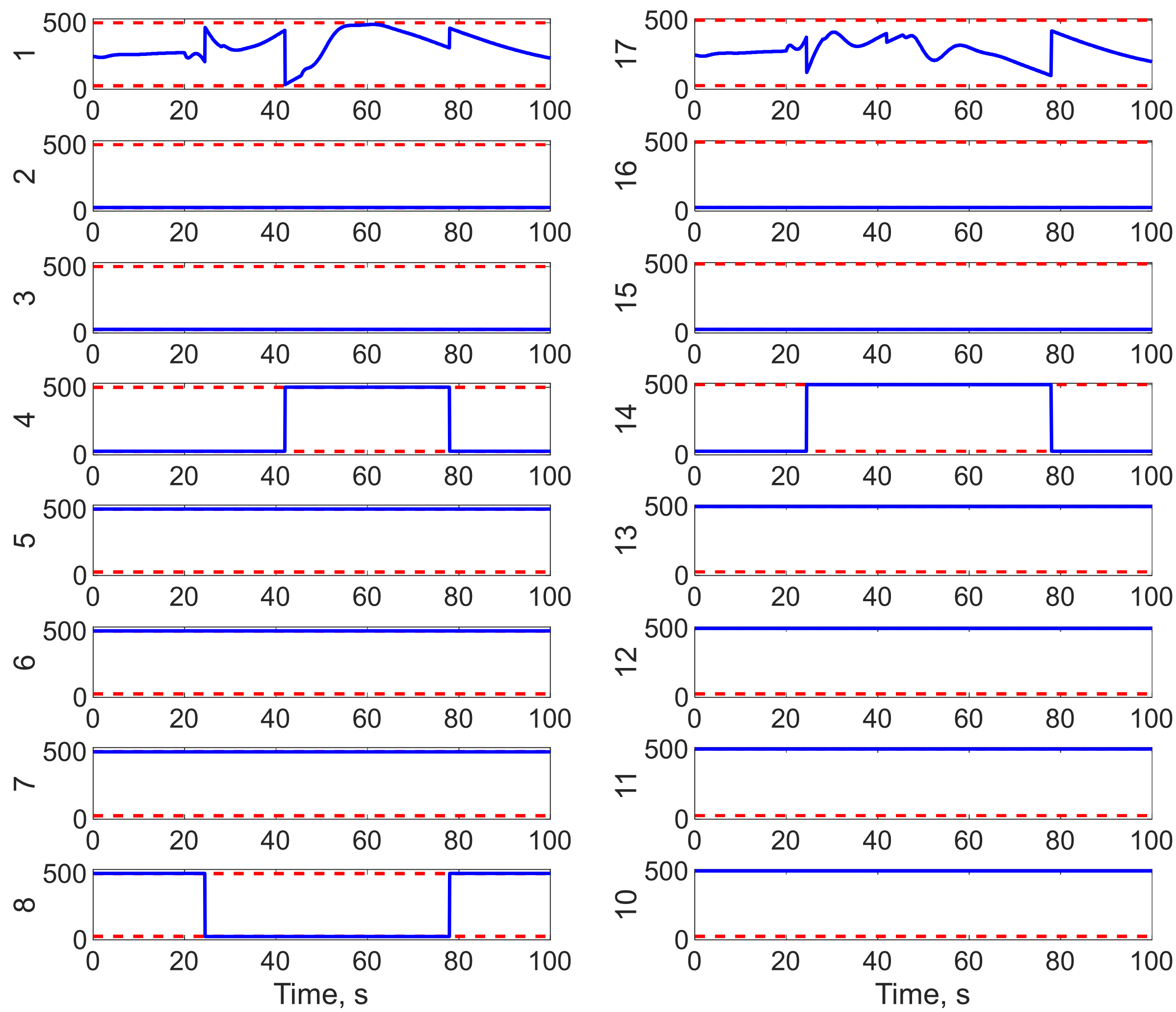

Figure 19. Example 3: Thrust commands for case using differential thrust to perform a coordinated turn. Numbered plots correspond to outermost to innermost wingfans top to bottom (refer to Figure 12). Dashed lines indicate upper (500 lbf) and lower (26 lbf) limits.

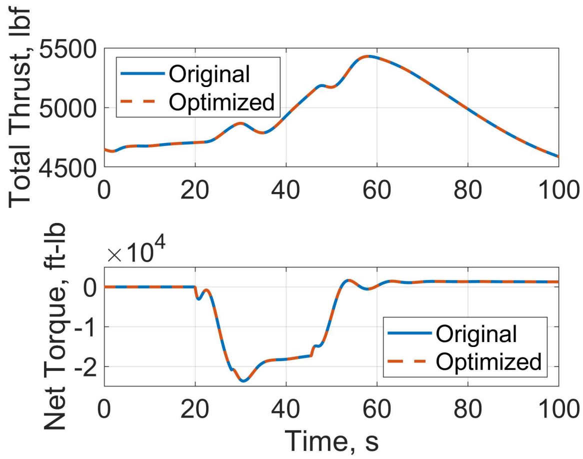

Figure 20. Example 3: Total thrust and net yaw axis torque due to original and optimized commands.

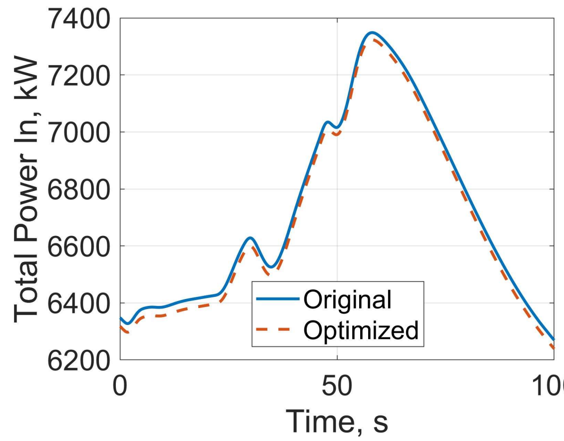

Figure 21. Example 3: Total input power for example with differential thrust.

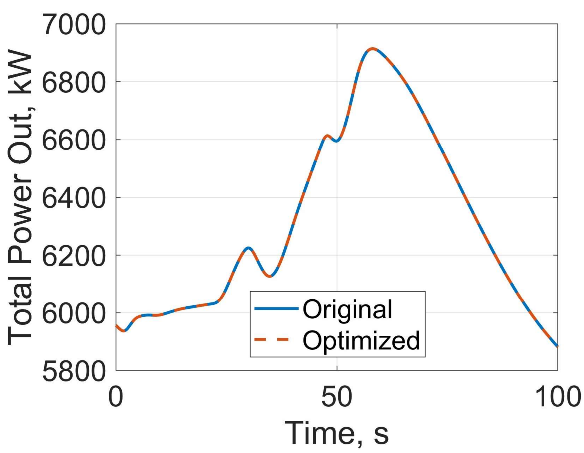

Figure 22. Example 3: Total output power for example with differential thrust.

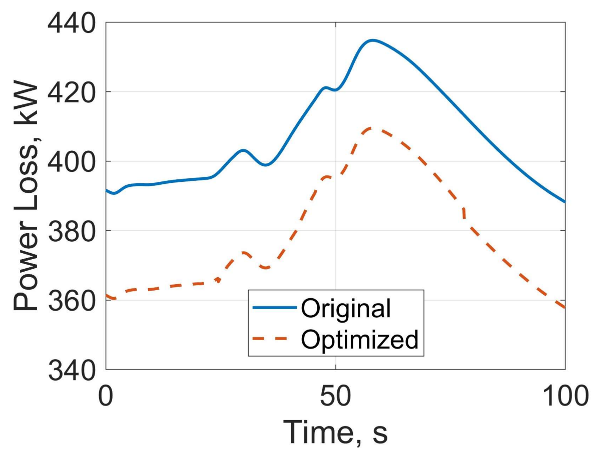

Figure 23. Example 3: Power loss for example with differential thrust.

of the thrust and the outermost pair provided whatever was unmet by the other 14. Here, because the net yaw axis torque was zero, the selection of fans was arbitrary, any sets of symmetrical pairs would work. Because of this, smoother (continuous) control could have been achieved by letting wingfans 1 and 17 remain saturated between about 46 and 73 s (Figure 13) and allowing one of the remaining idling pairs to meet the remaining thrust demand. The approach used is a design decision related to implementing differential thrust. The third example took the same approach of utilizing the innermost wingfans for thrust and the outermost for adjustments. This makes sense because the outermost pair has the most control authority for turning, but that does not necessarily result in the truly optimal solution, which is related to the thrust level of the fans. Figure 24 compares the power losses for the second and third examples. While the power loss in the cases that commanded all wingfans individually is nearly identical, the optimal cases demonstrated significantly more variation, though still slight in terms of overall power consumption. This can be understood by comparing the wingfan commands (Figure 13 and Figure 19) to the deviations in Figure 24, focusing on the events between about 40 and 80 s. Recall that the premise of the optimal approach is that operation at a combination of minimum and maximum thrust is more efficient than at intermediate thrust, even though overall thrust is the same. In Figure 13, 10 wingfans are at their upper limit during that time, and wingfans 1 and 17 are near their lower limit. In Figure 19, only 9 are at full power and another, #1, is very close, while #17 stays within the range of 98-423 lbf; it is never near a limit. The closer to a limit a fan operates, it is either more efficient or its power loss is minimized. Therefore, a different, strategically selected pair of wingfans performing the thrust and torque fine tuning at a particular instant might operate closer to their limits than the outermost pair would, and thus lose less power. However, extracting every bit of theoretical savings can add significantly to the complexity of the algorithm and to the wear and tear on the components. For the third example, several operational philosophies were investigated. One of these involved selecting wingfan pairs to act differentially based on the net yaw axis torque demand at a given instant. However, the rapid change in net yaw axis torque between about 23 and 30 s (Figure 20) caused fan setpoints to toggle back and forth between limits in less than a second. In the end, fewer setpoint jumps with the possibility of a negligible power penalty was deemed the more desirable solution.

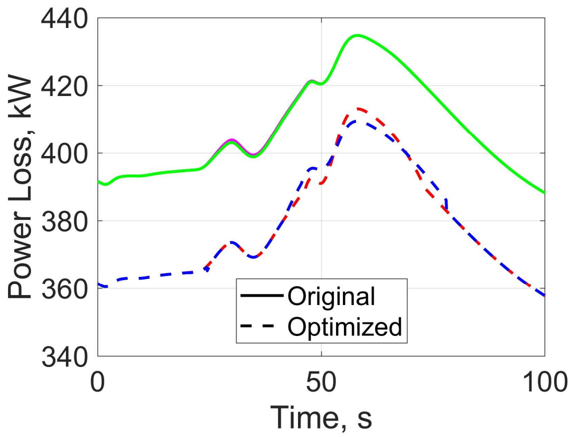

Figure 24. Power loss for the last two examples. Solid magenta (visible at around 30s) and dashed red for the zero net yaw axis torque example, solid green and dashed blue lines for the differential thrust example.

Looking at Figure 17 and Figure 23, around the point of highest power loss (about 58 s, which corresponds to the highest total thrust), the savings due to the optimal thrust commands are less than at other points in the examples. This is because in both cases 10 wingfans are essentially at full power (counting #1 in Figure 19) for a short time, while elsewhere fewer are at full power. The savings diminish and eventually disappear at very high and very low powers, since all fans are at similar thrust levels using either control approach. Still, as long as there is flexibility to adjust the commands, moving setpoints toward the limits will be beneficial because the power loss reduction on the low end will always exceed the power loss increase on the high end, assuming the efficiency curve increases monotonically, and its slope decreases with increased thrust. Figure 24 demonstrates this, showing a very slight decrease in power loss using the original (continuous) commands from the flight control [4] for the case with differential thrust compared to the case with zero net yaw axis torque (where all wingfan commands are the same) at about 30 s. This is the point at which the thrust commands separate widely, i.e., move toward the limits, for the coordinated turn (Figure 18). Although the total thrust is the same in the two cases, the differential thrust flight control commands result in more efficient operation.

It was mentioned earlier that rapid accelerations and decelerations of the fans can cause them to wear out prematurely. Additionally, it would be beneficial to alternate which fan pairs produce the majority of the thrust at mid-power settings to allow for even usage. There is also the concern of the batteries and bus being able to handle the power surges required for multiple simultaneous accelerations, even with the potential for regeneration upon deceleration. Finally, the example of differential thrust for turning occurred at a mid-power setting. Although it has been shown to be effective, the ability to use this technique at very high or very low power would be extremely limited. Given these limitations, the greatest benefit might be to use the optimal approach at steady state cruise conditions without differential thrust, avoiding rapid toggling of the fan setpoints.

The notional motor (and similar entire electrical string) map in Figure 2 bears further discussion, since the premise of the optimal solution depends on it. Compare it to Figure 25, which is also a common representation of a motor efficiency map, with its corresponding efficiency curve (Figure 26). Here, efficiency reduces slightly as the operation approaches the power limit boundary, meaning that the point of maximum power does not coincide with highest efficiency. This makes the problem slightly more complicated, but will not, in general, significantly change the result. As long as the difference in power level between the most efficient point on the operating line and the maximum power level is relatively small, toggling between idle and the most efficient point will be optimal in most cases. This reserves the highest individual fan power settings for cases with very high overall thrust demand, for which, as mentioned previously, little benefit can be realized.

VI. Conclusions

The optimal approach presented here is based on the observation that the point of highest efficiency of each of the components in the powertrain generally aligns, or at least that an end-to-end efficiency map has the characteristic of highest efficiency in the high torque/high speed region. Furthermore, it makes the assumption that the efficiency curve can be represented sufficiently well by a monotonically increasing function with decreasing slope. The former has strong empirical support; the latter is somewhat arbitrary, although, in general, component efficiency maps display a rate of change that becomes significantly more gradual from lower left to upper right. Using the assumed efficiency curve, the semi-bang-bang control scheme was shown to reduce power consumption compared to a continuous control method; the specific form of the efficiency curve is less important than the general property that it increases

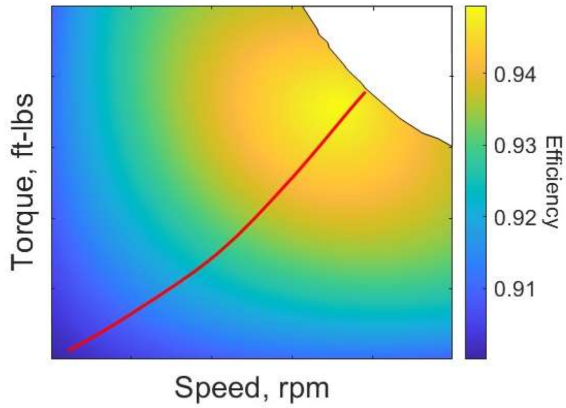

Figure 25.Notional motor efficiency map showing fan cruise operating line.

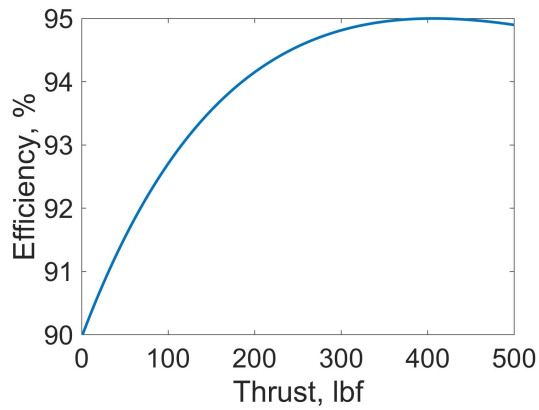

Figure 26. Notional efficiency plot corresponding to the map in Figure 25 for a cruise condition.

monotonically, at least until close to the maximum power boundary, while the slope decreases with increased thrust. Overall, the power savings must be weighed against the negative impacts of rapid acceleration and deceleration of the fans—effects such as motor life consumption and the ability of the batteries and bus to support the required power surges. Slower transitions between operating points for sustained steady state operation can eliminate the undesirable results with a negligible power consumption penalty.

Acknowledgments

This work is sponsored by the Transformational Tools and Technologies Project, which is part of the Transformative Aeronautics Concepts Program, under the NASA Aeronautics Research Mission Directorate.

References

[1] Jansen, R.H., Bowman, C.L., Clarke, S., et al., "NASA Electrified Aircraft Propulsion Efforts," Hybrid/Electric Aero-Propulsion Systems for Military Applications, NBR - 3 – 1, October 7-9, 2019, Trondheim, Norway.

[2] Kim, H.D., Perry, A.T., and Ansell, P.J., "A Review of Distributed Electric Propulsion Concepts for Air Vehicle Technology," AIAA 2018-4998, 2018 AIAA/IEEE Electric Aircraft Technologies Symposium, July 9-11, 2018, Cincinnati, OH.

[3] Sachs-Wetstone, J.J, Litt, J.S., Kratz, J.L., Buescher, H.E., "SUbsonic Single Aft eNgine (SUSAN) Power/Propulsion System Control Architecture Updates," AIAA-2024-1330, AIAA SciTech 2024 Forum, Orlando, FL, January 8-12, 2024.

[4] Litt, J.S., "Optimal Control Allocation for Distributed Electric Propulsion in a Series/Parallel Partial Hybrid Powertrain," Journal of Engineering for Gas Turbines and Power, Vol. 147, Issue 1, January 2025.

[5] Ogden, N.C., and Patterson, A. "A Framework for Evaluating Distributed Electric Propulsion on the SUSAN Electrofan Aircraft." NASA/TM–20230009523. July 2023.